Arch. Metall. Mater., Vol. 61 (2016), No 2, p. 559–568

DOI: 10.1515/amm-2016-0096

J. GUŚPIEL*, A. WIERZBICKA-MIERNIK*,#, W. RECZYŃSKI**

KINETICS OF CORROSION PROCESS IN H_2SO_4 AND HNO_3 AQUEOUS SOLUTIONS OF LEAD FREE Sn-Ag-Cu SOLDER ALLOYS

This paper presents the results of the corrosion resistance of Sn-Ag-Cu alloys in air-saturated aqueous solutions containing NO_3^-, SO_4^{2-} ions, whose concentration was equivalent to their contents in acid rains and in concentrations 10 – 100 times higher. The Ag, Cu and Sn concentrations in the corrosive media were determined using the Atomic Absorption Spectrometry. The specific dissolution rate and corrosion current were derived using the a rotating disc technique. The corrosion rate of Sn-Ag-Cu alloys depends on pH of the examined solutions and on the concentration of oxygen near the phase boundary. In the whole range of concentrations of the applied H_2SO_4 + HNO_3 mixtures of acids, the pure Sn was more corrosion resistant than eutectic alloy as well as the near eutectic one, following the sequence: Sn>Sn3.66Ag0.91Cu>3.8Ag0.7Cu.

Keywords: electronic materials; polarization; acid corrosion

1. Introduction

The most basic and universal solder materials used in electronic and electrotechnical industry until last years have been tin and lead alloys. Due to their high toxicity and growing awareness regarding the protection of environment and human health, a research has been launched to find replacement for the alloys used [1]. New materials, which should substitute the traditional tin-lead solders, need to meet some basic requirements regarding melting temperature, chemical composition (eutectic and near eutectic), wettability and surface tension, which should be similar to traditional tin-lead solder properties.

The corrosion of solids in aqueous solutions proceeds in few stages. The reactants must be transformed to the surface of the material as an effect of convection or diffusion, where they undergo a chemical transformation, and then the products leave the reaction area or precipitate on the surface of metal. The rate of the whole corrosion process is affected by its slowest stage.

The Sn-Ag-Cu (SAC) alloys of near - or of eutectic composition (3.66 wt% Ag and 0.91 wt% Cu [2]) are one of the most popular alloys . Although the metals contained in these alloys are not harmful to the environment or human heath in small quantities, when accumulated, they can become toxic (especially Cu and Sn), causing disorders in functions of humans and animals. Since the solder connections used in electronic utensils are often, dependently on their purpose, exposed to such factors as humidity, air pollution, sea water or acid rains, these factors cause or accelerate their degradation due to the corrosion processes. That is why it is important to determine the dissolution degree in the natural water environment for the materials from the SAC group.

New environment-friendly solder materials should not have a negative impact on human health and life [3] and should not undergo significant degradation caused by time and temperature changes, or other environmental factors.

In order to define the decisive stages, which mostly affect the rate of the investigated corrosion process of Sn-Ag-Cu type alloys, the rotating disc technique described in work [4] was used. The aqueous solutions of H_2SO_4 and HNO_3, in which NO_3^-, SO_4^{2-} ion concentrations, according to [5], were equivalent to those in acidic rains (solution A with pH = 4.5), and concentrations that corresponded to Ax10 (pH = 3.5), Ax50 (pH = 2.7) and Ax100 (pH = 2.46) have been used for kinetic research.

2. Experimental procedures

Alloys of two compositions (in wt%): Sn 95.43, Ag 3.66, Cu 0.91 eutectic alloy marked as S-1 and near eutectic Sn 95.5, Ag 3.8, Cu 0.7 one denoted as S-2 have been investigated.

Samples were prepared by using the following components: Ag and Sn of 99.999% and copper of 99.99% purity. Weighted amounts of metals were additionally deoxidized in the copper column and melted in the induction furnace [6] under 5N argon atmosphere to obtain cylindrical samples with the cross-section of 0.49 cm^2.

The samples were subjected to scanning electron microscopy examinations (EDS, XL-30 ESEM, FEI) to check the phase homogeneity and chemical composition.

Corrosion tests were carried out at 15 – 35 °C in air-saturated aqueous solutions with pH of 4.5 to 2.46, which contained ions NO_3^-, SO_4^{2-} of concentration equivalent to

* INSTITUTE OF METALLURGY AND MATERIALS SCIENCE, POLISH ACADEMY OF SCIENCES 25 REYMONTA STR., 30-059 KRAKOW, POLAND

** AGH UNIVERSITY OF SCIENCE AND TECHNOLOGY, FACULTY OF MATERIALS SCIENCE AND CERAMICS, AL. MICKIEWICZA 30., 30-059 KRAKOW, POLAND

Corresponding author: wierzbickamiernik@gmail.com

those in acid rains [5], and more concentrated solutions. The solutions were prepared using distilled water and analytical grade reagents: H_2SO_4, HNO_3. The exact compositions of solutions used are listed in Table 1.

TABLE 1

Composition of solutions used [mol/dm^3].

	H_2SO_4	HNO_3	pH
A	$2.32*10^{-5}$	$4.4*10^{-5}$	4.50
Ax10	$2.32*10^{-4}$	$4.4*10^{-4}$	3.50
Ax50	$1.16*10^{-3}$	$2.2*10^{-3}$	2.70
Ax100	$2.32*10^{-3}$	$4.4*10^{-3}$	2.46

The corrosion processes have been investigated using the rotating disc (RDE) technique. The rate of spontaneous dissolution of alloys in the aqueous solutions, electrochemical density of corrosion and limiting current measured at different speeds of stirring were determined.

2.1. Spontaneous dissolution of alloys

The alloy surfaces (0.49 cm^2) to be exposed to corrosive media were polished with grit 1000 water emery paper and then cleaned with filter paper. After polishing, the investigated alloys were firmly embedded into a cylinder shape teflon holder of 30 mm in diameter, whose shape assured the needed hydrodynamic conditions. Prepared in this way alloy surface was in the same plane as the Teflon cover. The measurements were performed in a glass cell containing 200 cm^3 of solution at temperatures 15.0 up to 35.0 ± 0.1 °C. Angular velocity of the disc was changed from 10.5 to 94.2 rad/s (100 to 900 rpm.). The rate of spontaneous dissolution of the alloys has been determined based on Sn, Ag and Cu concentration measurements in the investigated solutions.

These contents have been established with the atomic absorption spectrometry (ASA) method, flame technique and using acetylene air frame. In the case of Cu and Sn concentrations a HGA-600 (Perkin Elmer, USA prod.) instrument with a graphite dish was used. Additionally, in the case of Sn, the optimization of graphite dish work parameters has been conducted, using a „Method Development" program. The measurements have been carried out in a pyrolitic graphite dish, with L'vova platform. Taking into account chemical interferences, the formula modifier has been used (NH_4NO_3). Due to spectacular interferences, the deuter correction of the background has been applied. In each case the measurements have been performed with the formula of addition method.

The specific dissolution rate j [mol/cm^{2}s] was calculated by dividing the tangent of the slope angle of a straight line $M = f(t)$ by geometric disc surface area, where $M = (m_{Sn} + m_{Ag} + m_{Cu})$ is the sum of mole quantity of Sn, Ag and Cu transferred to the solution in time t at a given disc rotation speed.

2.2. Current density measurements

Measurements were carried out by a standard three-electrode measuring system: platinum as the counter electrode, Sn-Ag-Cu alloy as the working electrode and a saturated calomel electrode, SCE, as the reference with a Luggin capillary bridge connected to the test solution. The distance between the working electrode and the counter electrode was about 50 mm.

The working electrodes were firmly embedded into a cylindrical Teflon holder (see section 2.1) with a brass contact with the meters. The surface of the alloy was prepared accordingly to the standards used during the spontaneous dissolution of alloys.

The measurements were performed in a glass cell containing 600 cm^3 of solution. Angular velocity of the disc was changed from 80 to 670 rpm (8.3 to 69.8 rad/s). The measurements were carried out at room temperature (25.0 ± 0.1 °C).

During the potentiodynamic polarization tests, the working electrode was scanned from the cathodic to anodic polarization state in the potential range from -150 mV to +200 mV versus OCP at the scan rate of 1 mV/s. Corrosion current density was calculated from fitting of the Butler-Volmer equation to the experimental data using NOVA software for *i/E* analysis [7,8].

The $I = f(\omega^{1/2})$ and the limiting currents of oxygen cathodic reduction measurements were performed using the rotating disc electrode (RDE).

During the potentiostatic measurements the $I = f(\omega^{1/2})$ relation was determined by measuring the value of the anode current for the potential of + 20 mV versus OCP, at ω = const. Before each measurement the samples were treated for 600 s in the test solution.

During the measurements, the limiting currents of oxygen cathodic reduction and potentiodynamic polarization curves $I = f(E)$ at ω = const were determined in the range from -1300 mV to E_{corr} range at scan rate 1 mV/s or 10 mV/s.

All measurements were carried out by applying the potentiostat Autolab PGSTAT 302 .

3. Results

3.1. Open circuit potential

Fig. 1 shows the evolution of the open circuit potential (OCP) for Sn, eutectic (S-1) and near eutectic (S-2) alloys. During the first 600 s from the time of immersion of alloys in the solution, the OCP potential increased to the values corresponding to the more noble ones. After this time, during the next 1800 s the OCP value has slightly changed.

Therefore, in order to obtain comparable corrosion test conditions, during the anodic current density measurements, before each measurement, the samples were treated for 600 s in the test solution.

The positive shift of the potential is probably due to the development of a certain passive film on the metal surface [9,10].

The similar effect of the OCP measurements was described by El-Taib Heakal et. al. [9] for the corrosion of Sn-Ag alloys in the 0.075 – 4.5 M solution of HNO_3.

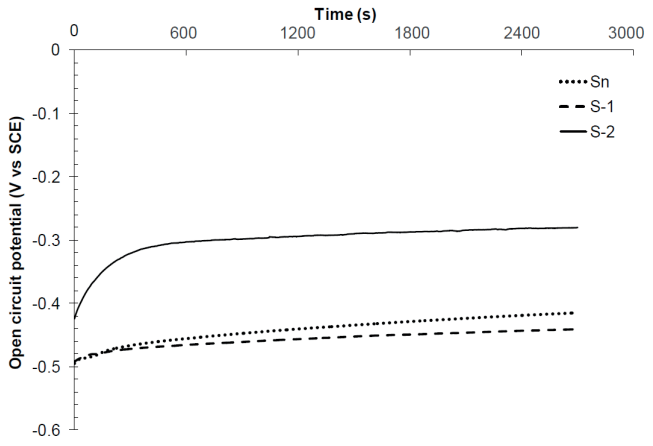

Fig. 1. Evolution of the open circuit potential OCP for Sn and S-1, S-2 alloys in A type solution at 25 °C

3.2. Corrosion potential and corrosion current density in unstirred solution

The Fig. 2 presents the relationships of log *(/I/) = f(E)* for Sn, S-1 and S-2 alloys in A type unstirred solution, which were used to determine the value of the corrosion potential E_{corr} and current density values I_{corr} calculated from fitting of the Butler-Volmer equation to the experimental data using NOVA software for *log i = f(E)* analysis [7,8].

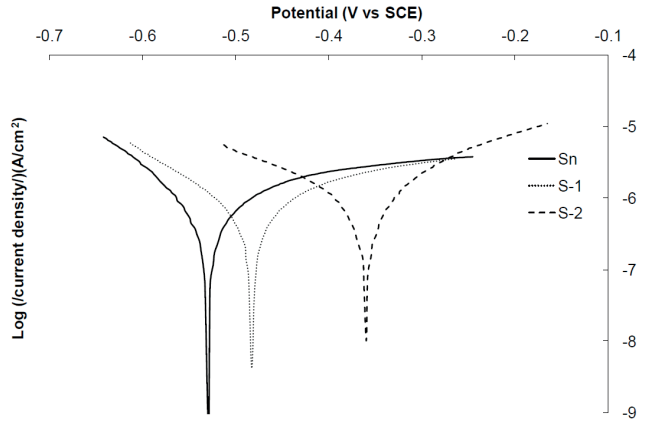

Fig. 2. Potentiodynamic polarization curves *log* (*/I/*)=*f*(*E*) of Sn and S-1, S-2 alloys in A type unstirred solution at 25 °C

TABLE 2

Potentiodynamic measurement results

Type of samples	E_{corr} [V]	I_{corr} [A/cm^2]
Sn	-0.530	0.82 *10^{-6}
S-1 (Sn3.66Ag0.91Cu)	-0.482	0.91*10^{-6}
S-2 (Sn3.8Ag0.7Cu)	-0.362	1.38*10^{-6}

3.3. Cathodic branch of polarization curves

The polarization curves are shown in Figs. 3a and 3b, where *I = f(E)* is determined for the eutectic (S-1) alloy and near eutectic (S-2) (respectively) in the solution Ax50 by the rotating disc technique (RDE) at various rotation speeds; the curves were recorded from negative potential *E* = -1300 mV to the corrosion potential $E_{corr.}$

Limiting current values I_{lim}, for potential -1 V, and for various values of ω are shown in Fig. 4.

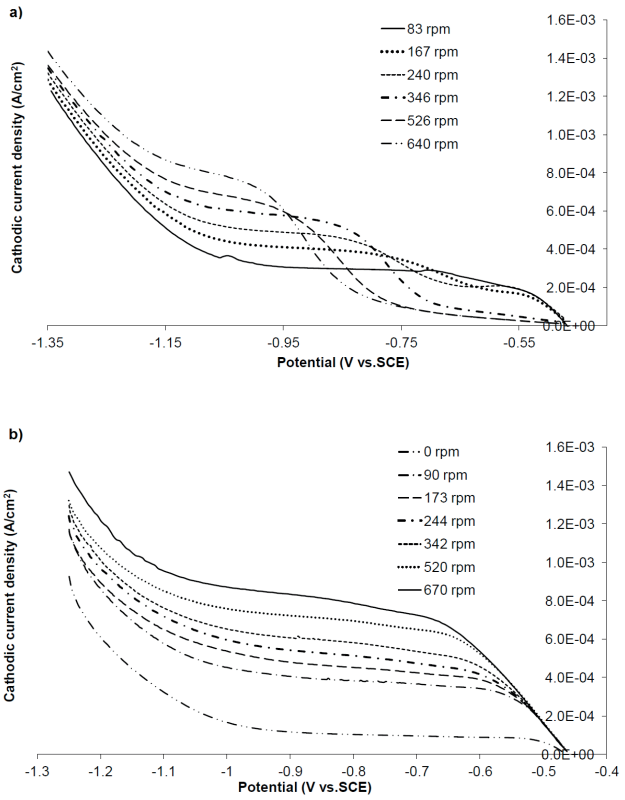

Fig. 3. Potentiodynamic polarization curves of S-1 and S-2 alloy in Ax50 solution for ω from 0 rpm to 670 rpm, and at scan rate: 10 mV/s (a) and 1 mV/s (b)

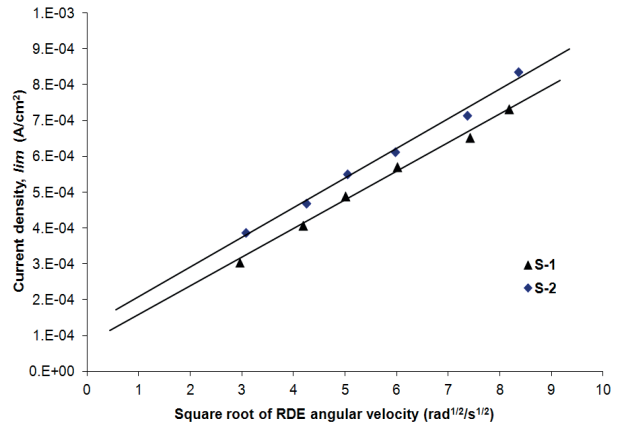

Fig. 4. Plot of current density as a function of rotation rate at potential -1 V for S-1, S-2 alloys in Ax50 solution

Data points shown above (Fig. 4) (using the data presented in Figs. 3a and Fig.3b at potential -1000 mV) follow straight line equation: $I = 8*10^{-5}\ \omega^{1/2} + 0.8*10^{-4}$ [A/cm^2] *and* $I = 8*10^{-5}\ \omega^{1/2} + 1.2*10^{-4}$ [A/cm^2], respectively. The linear correlation for the relation $I = f(\omega^{1/2})$ in the case of the experimental data is above 99.9 %.

The straight line does not cross the origin which suggests, that the measured total value of the current was a sum of two corrosion reactions $I = I_{lim} + I_r$: the inhibited activation – this non-diffusion component of the current is approximately $I_r = 0.8*10^{-4}$ [A/cm^2] (S-1) or $I_r = 1.2*10^{-4}$ [A/cm^2] (S-2) and I_{lim} is the same: $I_{lim} = 8*10^{-5}\ \omega^{1/2}$, which affects the diffusion control of the cathodic reaction. The possible course of this diffusion and non-diffusion component is discussed in part 4. The similar effect, i.e. the presence of non-diffusion component of the current, has been reported in work [11].

3.4. Kinetics of corrosion reaction

3.4.1. Current density measurements

The results of the electrochemical measurements derived by rotating disk technique (RDE) are shown in Figs. 5, 6 and 7.

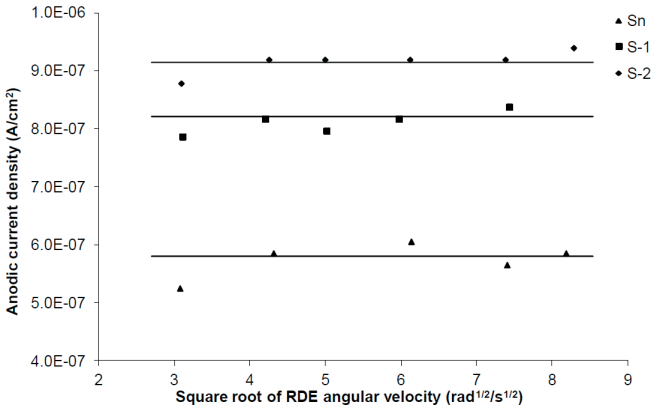

Fig. 5. Dependence of anodic current density $I_a = f(\omega^{1/2})$ for alloys S-2, S-1 and Sn in A type solutions at 25 °C

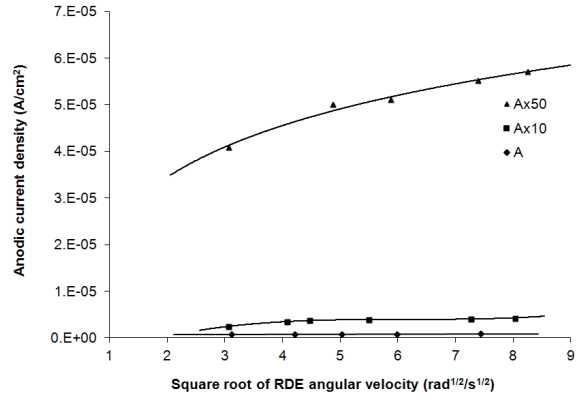

Fig. 6. Dependence of anodic current density $I_a = f(\omega^{1/2})$ for S-1 alloy in Ax50, Ax10 and A type solutions at ambient temperature (25 °C)

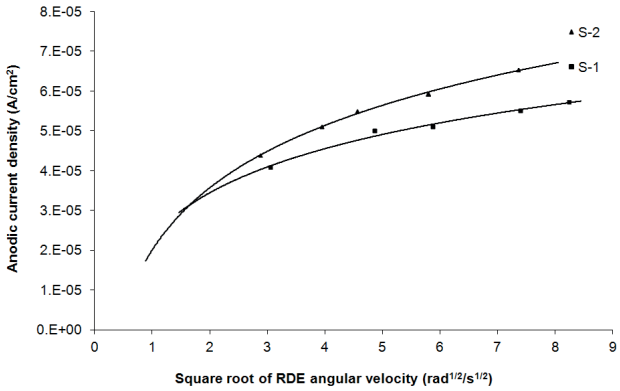

Fig. 7. Dependence of anodic current density $I_a = f(\omega^{1/2})$ for S-1 and S-2 alloy versus square root RDE angular velocity in Ax50 type solution at 25 °C

The shape of the curves shown in Fig. 5, suggested that the corrosion process takes place in activation region, where there was no visible dependence of Ia on the rotation speed. In this range the rate of corrosion process was defined by the rate of the processes taking place on the interphase. This rate was at least few times lower than the transport velocity of reactants.

The shape of the curves shown in Fig. 6, suggested the transfer of the corrosion process from the activation region (solution A; pH = 4.50; Fig. 9) to the mixed region (solution Ax50; pH = 2.7; Figs. 6, 7). The observed change of reaction regions takes place when the concentration of H^+ ions in the solution increases. In the transitional region (e.g. for the Ax10 solution) of the curve $I_a = f(\omega^{1/2})$ after exceeding 20.8 rad/s (200 rpm), the velocity reached the value, above which the measured corrosion current density attains the limiting value (surface reaction rate), which was independent on the further increase of solution mixing speed.

In order to eliminate the oxygen from air-saturated solution with the concentration of Ax50 (mixed region) the solution was de-aerated with N_2 for 1 h prior the measurement. This allowed to shift the process into the activation region and to allow the direct measurement of the rate of anodic processes occurring on the surface of the alloy I_a. The measured value of I_a correlates with the value resulting from the dependence $I = f(\omega^{1/2})$, and is presented in Fig. 8.

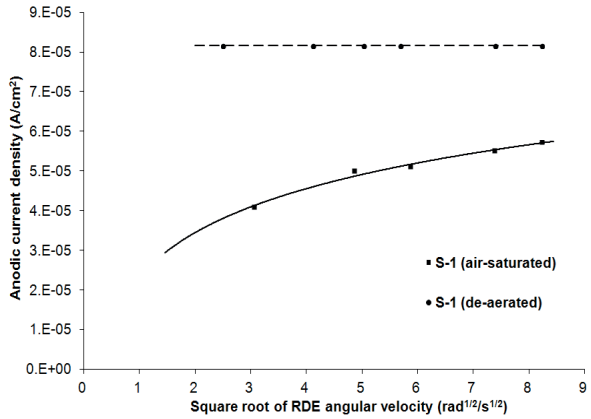

Fig. 8. Dependence of anodic current density $I_a = f(\omega^{1/2})$ for S-1 alloy versus square root RDE angular velocity at 25 °C in Ax50 type solution air-saturated and de-aerated

The values regarding the surface reaction rate of S-1 alloy, defined in the experimental way are shown below (Fig. 9):

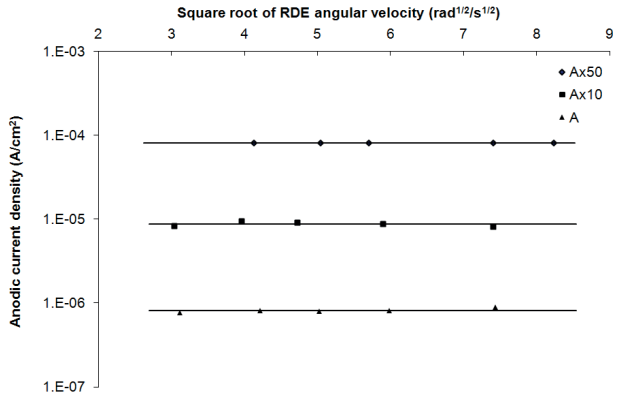

Fig. 9. Dependence of surface reaction rate $I_a = f(\omega^{1/2})$ for S-1 alloy versus square root RDE angular velocity in Ax50 (de-aerated), and air-saturated: Ax10 and A type solution, at 25 °C

3.4.2 Spontaneous dissolution of alloys

The exemplary dependence of $M_{Me} = f(t)$ is shown in Fig. 10, which reflected the increase of the concentration of alloy elements in the solution as a function of time, with the curve presenting the concentration of Sn, Ag and Cu in the solution as a function of time. In each case the character of the above mentioned dependence was similar. At the beginning, for 15-20 minutes, the alloy dissolution speed was very low. After this period of time the dissolution speed was constant, for a given disc rotation speed. Since the Sn-Ag-Cu alloy dissolution rate was within the error margin corresponding with the rate of Sn transfer to the solution.

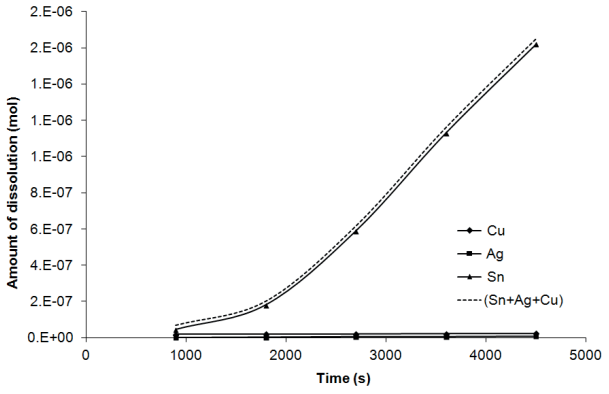

Fig. 10. Dependence of $M_{Me} = f(t)$ for Sn, Ag, Cu determined in Ax100 solution at 25 °C and ω= 110 rpm

The exemplary dependencies $M = f(t)$, presenting the rate of dissolution of eutectic (S-1) alloy as a function of time for the given disc rotation speeds, are shown in Fig. 11.

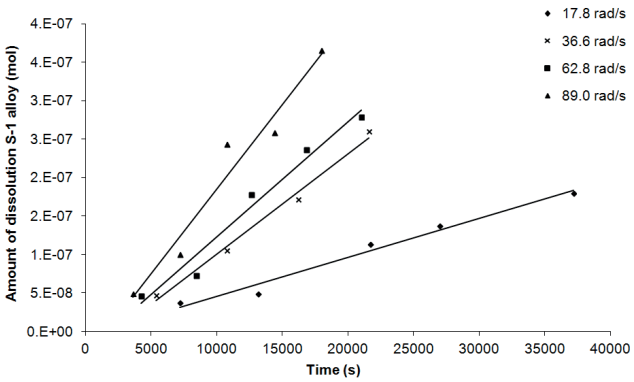

Fig.11. $M = f(t)$ dependency for S-1alloy in Ax50 solution at T = 25 °C and ω = const

In all cases the $M = f(t)$ dependencies were depicted by straight lines, with the probability of linear correlation over 99%.

The straight lines did not intersect at the beginning of the coordinate system, because of significantly low rate of alloy dissolution during first 15 - 20 minutes. After this time, the rate of dissolution was constant in time, for the given disc rotation speed. The specific dissolution rate j [mol/cm^{2}s] was calculated by dividing the tangent of the slope angle of straight line $M=(m_{Sn}+m_{Ag}+m_{Cu})t = (\Delta m/\Delta t)t$ [mol] by the geometric disc surface area (S).

$$j=(\Delta m/\Delta t)/S \quad [\text{mol/cm}^2\ \text{s}] \qquad (1)$$

The results of the measurements are shown in Figs. 12 - 15.

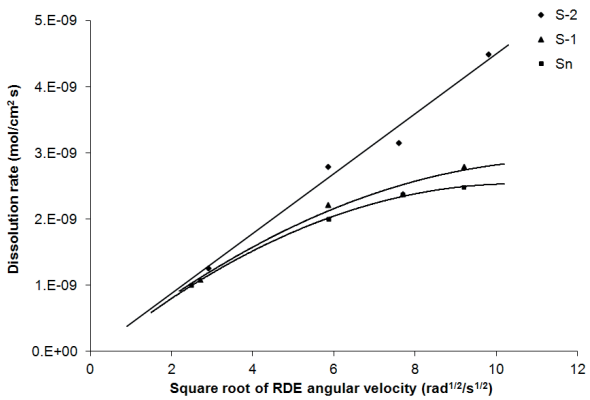

Fig. 12. Plot of specific dissolution rate for S-1, S-2 alloys and Sn versus square root RDE angular velocity at T = 25 °C in Ax100 solution

The straight line obtained for the dependence of the corrosion rate and disc rotation speed obtained for the S-2 alloy, crossed the origin of coordinates and is characteristic for the dissolution process in the diffusion region, in which, according to the Levich theory [4], the diffusion rate depends on the slowest flux of ions taking part in the reaction.

The value of the apparent activation energy determined according to equation (2) in the temperature range of 25 – 35 °C equals to E_a = 13.8 kJ/mol (Fig.13) is also characteristic for the dissolution process in the diffusion region, which confirms the above conclusion.

$$E_a=log(j_1/j_2)*2{,}303*R*((T_1*T_2/(T_2-T_1)) \qquad (2)$$

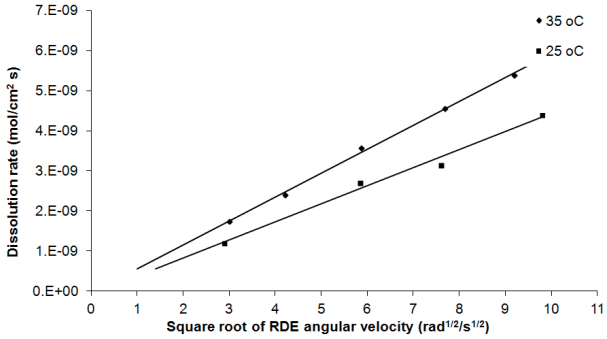

Fig. 13. Plot of specific dissolution rate for near eutectic (S-2) alloy in dependence on square root RDE angular velocity in the Ax100 type solution for: T = 25 °C and T = 35 °C

In the case of S-1 alloy and Sn at temperature 25 °C the curves monotonically decreased in the direction of growing $\omega^{1/2}$ values. Their shape suggested the course of dissolution in mixed kinetics region, in which, at the phase boundary diffusion flux can be compared with the rate of chemical reactions. The apparent activation energy value of S-1 alloy equaled $E_{a(15\text{-}25\ C)}$ = 24 kJ/mol and is characteristic for the mixed regions (Fig. 14).

With the increase of solution temperature from 25 °C to 35 °C the change of the type of dissolution process from the mixed regions to diffusion area was attained, which confirms the linear dependence of $j(\omega^{1/2})$ (Fig. 14) at 35 °C.

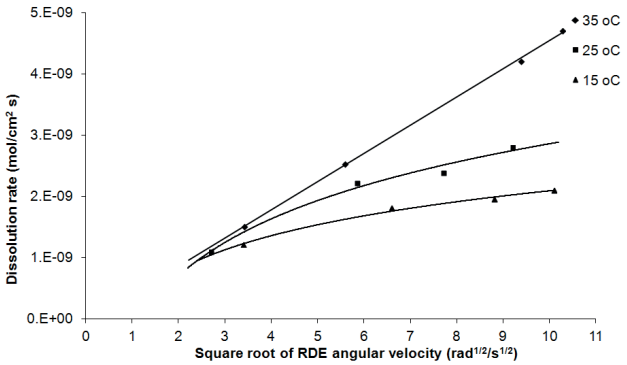

Fig. 14. Plot of specific dissolution rate for eutectic (S-1) alloy as dependence on square root RDE angular velocity in Ax100 type solutions at T = 15 °C, 25 °C and 35 °C

Similar dependencies $j=f(\omega^{1/2})$ were obtained in the Ax50 solutions (Fig. 15).

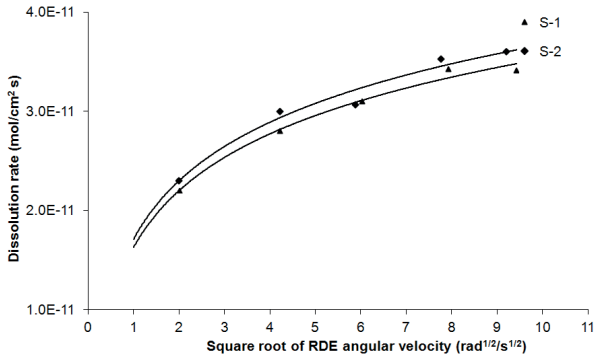

Fig. 15. Plot of specific dissolution rate for S-1 and S-2 alloy versus square root RDE angular velocity in Ax50 type solution at 25 °C

In the solution with the concentration of A and Ax10 the spontaneous dissolution was too slow to determine the corrosion rate based on measurements of Sn, Ag, and Cu ion concentration in the solution as a function of time. Therefore, in the case of those solutions, the corrosion rate was determined based on anodic current density measurements (see above).

Evaluation of the corrosion rate based on the current density measurements is much faster method than the measurement related to the spontaneous dissolution of the alloys taking into account the Sn, Ag and Cu concentration in the investigated solutions. The spontaneous dissolution method, although slower, allows in the most objective way to follow the progress of corrosion over time. Fig. 16 shows the comparison of the results of measured the corrosion rate obtained with both methods. The values of anodic current density I_a [A/cm^2] (Fig.7) were calculated for specific dissolution rate j [mol/cm^2 s] using the dependency (3), given below:

$$j=I_a/nF \qquad (3)$$

where n is the number of electrons involved in the reaction, and F stands for Faraday's constant.

For the calculation, the following values were used: n = 4; F = 96450 C/mol (see section 4)

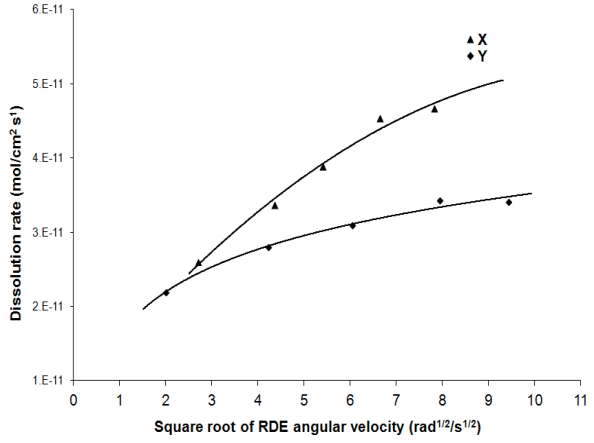

Fig. 16. Plot of specific dissolution rate for S-1 alloy versus square root RDE angular velocity in Ax50 type solution at 25 °C. ***X*** - specific dissolution rate calculated from the anodic current density measurements (Fig. 7), ***Y*** - spontaneous dissolution rate

The trend of the curves presented in Fig. 16 shows good agreement between the results obtained using two independent methods used for evaluation of corrosion process kinetics.

4. Discussion of the results

It is known, that for the most frequent case of a divalent metal, the corrosion reaction takes place with so called hydrogen depolarization according to the scheme below:

$$Me + 2H^+ = Me^{2+} + H_2 \qquad (4)$$

In the solutions that contain oxygen the corrosion proceeds with so called oxygen depolarization:

$$2Me + O_2 + 4H^+ = 2Me^{2+} + 2H_2O \qquad (5)$$

It is also possible that the reactions (4) and (5) run parallel.

Since the Sn-Ag-Cu alloy dissolution rate was within the error margin corresponding with the rate of Sn transfer to the solution (Fig. 10), it can be assumed for simplification, that in the examined solutions the main reaction affecting the corrosion rate was as follows (3):

$$2Sn + O_2 + 4H+ = 2Sn^{2+} + 2H_2O \qquad (6)$$

If either the transport of ions in the reaction region or the diffusion of the reaction products into the solution is the slowest stage of the corrosion process, then in the case of rotating disc electrode the rate of the process is described by Levich equation [4]:

$$j = 0.62\, D_i^{2/3}\, \nu^{-1/6}\, (C^o_i - C^l_i)\, \omega^{1/2} = k\,(C^l_i)^p \qquad (7)$$

where:
D - stands for the diffusion coefficient [cm^2/s], ν - stands for the solution viscosity [cm^2/s], C^o_i – is the bulk concentration of the reagent [mol/cm^3], C^l_i – is the concentration of the reagent at the surface of rotating disc electrode [mol/cm^3], ω - angular velocity [rad/s], k – constant of reaction, p – order of reaction.

If the corrosion process takes place in diffusion region $C^l_i \rightarrow 0$, the equation (7) gives the possibility of estimating the speed of ions' diffusion which takes part in the corrosion reaction.

The linear dependence of $j = f(\omega^{1/2})$ obtained for alloy S-2 in the Ax100 solution as an effect of spontaneous dissolution of alloys (Fig. 12) suggested the decrease of the corrosion rate, whose course is described by the equation $j_{lim} = (4.5 \pm 0.8)*10^{-10}\ \omega^{1/2} \approx j_{lim},Sn^{2+}$

according to reaction (6):

$$j_{O2} = \tfrac{1}{2}\, j_{Sn}^{2+} = \tfrac{1}{4}\, j_{H+} \qquad [\text{mol/cm}^2\,\text{s}] \qquad (9)$$

$$j_{lim,O2} = \tfrac{1}{2}\, j_{Sn}^{2+} = (2.25 \pm 0.42)*10^{-10}\ \omega^{1/2} \quad \text{– experimental data (Fig. 12)} \qquad (10)$$

$$j_{lim,O2} = 1.97*10^{-10}\ \omega^{1/2} \quad \text{- limiting flux of } O_2 \text{ reduction, according to the Levich equation (7)} \qquad (11)$$

The following parameters were used in calculations $j_{lim,O2}$, at 25°C: $D = 2*10^{-5}$ cm^2/s, $\nu = 10^{-2}$ cm^2/s, $C^0 = 2*10^{-7}$ mol/cm^3, ω [rad/s] [12].

Similar results were obtained measuring directly limiting current of oxygen reduction in solution Ax50 (Figs. 3, 4). Data points shown above (section 3.2. – Fig. 4) follow straight line equation: $I = 8*10^{-5}\ \omega^{1/2} + 0.8*10^{-4}$ [A/cm^2] (S-1) and $I = 8*10^{-5}\ \omega^{1/2} + 1.2*10^{-4}$ [A/cm^2] (S-2).

The experimental data are shown in Fig. 17, where non-diffusion component

$I_r = 0.8*10^{-4}$ and $I_r = 1.2*10^{-4}$ was subtracted from the total current and the diffusion flux equals $I_{lim} = 8*10^{-5}\ \omega^{1/2}$ [A/cm^2] is the same for S-1 and S-2 samples. The limiting current is according to the relation (7) and (3) $I_{lim} = nF\ 0.62nFD^{2/3}\nu^{1/6}C^0\ \omega^{1/2}$. The following parameters of the electroreduction of air oxygen were used in calculations $I_{lim,O2}$, at 298 K: $n = 4$, $F = 96450$ C/mol, $D = 2*10^{-5}$ cm^2/s, $\nu = 10^{-2}$ cm^2/s, $C^0 = 2*10^{-7}$ mol/cm^3, ω [rad/s] [12]. The result of calculations are as follows: $I_{lim,O2} = 7.6*10^{-5}\ \omega^{1/2}$ A/cm^2 (Fig.17).

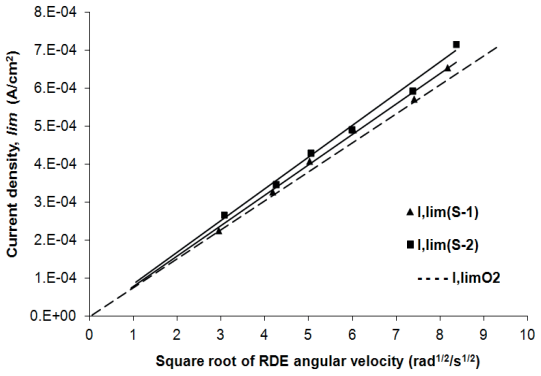

Fig.17. Plot of current density $I_{lim(S-1)}$, $I_{lim(S-2)}$, (experimental data) and $I_{lim,O2}$ (result of calculations) as a function of rotation rate

The good correspondence between the experimental and calculated data indicated that the limiting current was caused by a slow oxygen transfer from the bulk solution to the sample surface. It also meant that the cathodic branch of polarization curves might be ascribed to the dissolved oxygen reduction in the 4-electron transfer reaction.

The experimentally measured dissolution rate of the S-2 alloy ($j_{lim,O2} = (2.25 \pm 0.42)*10^{-10}\omega^{1/2}$) (Fig.12) is in good agreement with the experimentally determined limiting current of the electroreduction of oxygen ($j_{lim,O2} = j_{lim}/4F = 2.07*10^{-10}\ \omega^{1/2}$ - potentiodynamic measurements) (Fig. 17). This rate is also consistent with the theoretically calculated value according to the Levich equation (7) ($j_{lim,O2} = 1.97*10^{-10}\omega^{1/2}$). The results clearly show that in the case of Ax100 solutions the corrosion rate of the tested samples is determined by the rate of diffusion of oxygen dissolved in the solution. The rate of surface reaction in these solutions is much higher than the speed of oxygen diffusion flux.

In the Ax50 solutions the rate of surface reaction is comparable with O_2 diffusion speed, what suggests an activation-diffusional control of the dissolution rate.

In the case of A type solution, in the whole range of the applied speeds of the disc rotation the value of corrosion rate was independent of the speed of stirring the solution (Fig. 6). It means that corrosion proceeds in the activation area, and the speed of this process is determined by the speed of its physico-chemical processes occurring on the surface of the alloy. The change of the reaction area, observed with the change of pH values, (transfer from the diffusion region (pH = 2.46) (Fig. 12) through the mixed region (pH = 2.5) (Figs. 7, 15) to the activation one (Ax10 pH = 3.5; A pH = 4.5) (Figs. 5, 6) suggests a clear dependence of surface reaction rate on the concentration of hydrogen ions in the solution.

The analysis of $I_{lim} = f(\omega^{1/2})$ dependence (Fig. 4) (non-diffusion component of the current is approximately $I_r = 8*10^{-5}$ A/cm^2) suggests, that the corrosion in these solutions proceeds with simultaneous oxygen and hydrogen depolarization i.e. the reactions (4) and (5) run parallel.

The values (Fig. 9) regarding the surface reaction rate of S-1 alloy, defined in the experimental way are given below and shown in Fig.18:

Solution Ax50 (pH=2,7; $C^o_{H^+}=2.00*10^{-6}$ mol/cm^3) $I=8.16*10^{-5}$ A/cm^2

Solution Ax10 (pH=3.5; $C^o_{H^+}=3.16*10^{-7}$ mol/cm^3) $I=8.82*10^{-6}$ A/cm^2 (12)

Solution A (pH=4.5; $C^o_{H^+}=3.16*10^{-8}$ mol/cm^3) $I=8.20*10^{-7}$ A/cm^2

where $I = nFk\,(C^o_{H+})^p$

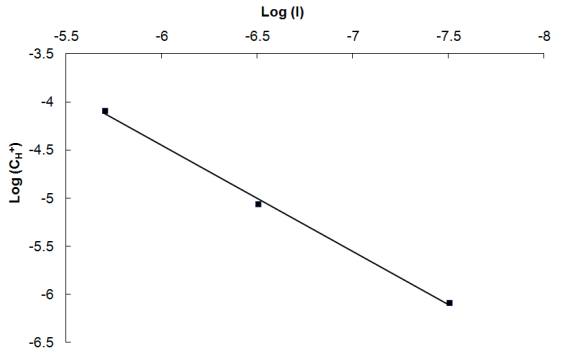

Fig.18. Dependence of $log(I)=f(log(C_{H^+}))$ for S-1 alloy in Ax50, Ax10 and A type solution at 25 °C

The result of calculations with the equation (12), leads to the conclusion, that the surface reaction is of first-order (p = 1) for the concentration of hydrogen ions H^+ in the solution calculated from pH data.

The detailed description of the analysis of the experimental data, that were obtained by rotating disc electrode can be found in Zembura's [12] and Guspiel's [13,14] works.

The shift of E_{corr} to less negative values was observed with the increase of Ag content in the alloy, following the sequence: Sn<S-1<S-2 with the simultaneous increase of the corrosion current (Fig. 2; Table 2). This apparent contradiction is probably due to the several reasons:

- the addition of the more noble elements (Ag and Cu) into pure tin, affects the shift of E_{corr} towards more positive values,
- pure tin is the most resistant due to its high ability to partial passivation of the samples. It was most probably due to the SnO formation [15,16], and its amount was strictly related to the amount of βSn phase in the samples (increasing in the sequence S-2, S-1 and Sn). Therefore, the longest passivation stage was observed for pure tin, a shorter one for S-1 and the shortest for the S-2 alloy (Fig. 2) [15],
- the differences in the corrosion rate between S-1 and S-2 (S-2>S-1) alloys can be related to the amount of the Ag_3Sn phase in the alloy (more noble then the βSn phase), which in the electrochemical reactions acted as a cathode and promoted the dissolution of the βSn phase (anode) [16].

5. Conclusions

The results regarding the dissolution rate of Sn3.66Ag 0.91Cu (eutectic) and Sn3.8Ag0.7Cu alloys in the mixture of oxygen-saturated H_2SO_4 + HNO_3 of different pH values lead to the conclusions as below:

1. In the whole range of concentrations of used H_2SO_4 + HNO_3 acids mixtures, including those where the NO^3, SO_4^{2-} ion concentrations were equivalent to those in acid rains (solution A with pH=4.5), the pure Sn was more corrosion resistant than eutectic alloy as well as the near eutectic one, following the sequence: Sn> S3.66Ag0.91Cu> Sn3.8Ag0.7Cu
2. In the solutions, in which pH < 3 the dissolution process occurs in the diffusion region or mixed region, and its rate depends on the rate of oxygen diffusion, transferred to the reaction surface. It increases with the intensity of mixing.
3. In the solutions with pH > 4, the corrosion rate does not depend on the intensity of stirring and the rate of diffusion of oxygen towards the alloy surface. The corrosion rate is determined by the rate of anodic reaction on the surface. The rate of the reaction is influenced by the concentration of hydrogen ions in the solution, and the increase of their concentration accelerates the rate of corrosion.

Acknowledgements

The research was financially supported by the Polish Ministry of Science and Higher Education under the Grant N N507 443734.

REFERENCES

[1] 'Directive on the restriction of the use of certain hazardous substances in electrical and electronic equipment', Directive 2002/95/EC, Official Journal of European Union, 13 February 2003.

[2] Data Base for Properties of Lead-Free Solder Alloys, version 1.0, Database is a joint project of ELFNET and COST 531

Action.
[3] A. Watson, L. Zabdyr, Thermodynamic Approach to Modern Alloy Design, Foundation of Materials Design, Recent Research Developments in Materials Science, Research Signpost, Trivondrum, Kerala Indiá, (2006).
[4] V.G. Levich, Physicochemical Hydrodynamice. Presntice_ Hall, New Jersey, N.J. (1962).
[5] B. Walna, J. Siepak, Sci. Total. Environ. **239**, 173 (1999).
[6] [6] A. Sypien, W. Przybylo, J. Mater. Sci. Technol. **26**(1), 31 (2010).
[7] A.J. Bard L.R. Faulkner, Electrochemical methods, second ed., Wiley, New York (2001).
[8] J.O. Bockris, A.K.N. Reddy, Modern Electrochemistry **2**, 883 (1977), Plenum press, New York.
[9] F. El-Taib Heakal, A.M.Fekry, A.A.Ghoneim, Corros. Sci. **50**, 1618 (2008).
[10] M. Mori, K.Miura, T. Sasaki, T. Ohtsuka, Corros. Sci. **44**, 887 (2002).
[11] [11] A.P. Yadav, A. Nishikata, T. Tsuru, J. Electroanal. Chem. **585**, 142 (2005).
[12] Z. Zembura, A. Fuliński, Electrochim. Acta **10**, 859 (1965).
[13] J. Guspiel, W. Riesenkampf, Hydrometallurgy **34**, 203 (1993).
[14] J. Guspiel, Physicochem. Problems Mineral. Proc. **31**, 107 (1997).
[15] A. Wierzbicka-Miernik, J. Guspiel, L. Zabdyr, Arch. Civ. Mech. Eng. **15**, 206 (2015).
[16] F. Rosalbino, E. Angelini, G. Zanicchi, R. Marazza, Mater. Chem. Phys **109**, 386 (2008).